



## City Research Online

### City, University of London Institutional Repository

---

**Citation:** Mergos, P.E. (2023). Sustainable and resilient seismic design of reinforced concrete frames with rocking isolation on spread footings. *Engineering Structures*, 292, 116605. doi: 10.1016/j.engstruct.2023.116605

This is the accepted version of the paper.

This version of the publication may differ from the final published version.

---

**Permanent repository link:** <https://openaccess.city.ac.uk/id/eprint/30990/>

**Link to published version:** <https://doi.org/10.1016/j.engstruct.2023.116605>

**Copyright:** City Research Online aims to make research outputs of City, University of London available to a wider audience. Copyright and Moral Rights remain with the author(s) and/or copyright holders. URLs from City Research Online may be freely distributed and linked to.

**Reuse:** Copies of full items can be used for personal research or study, educational, or not-for-profit purposes without prior permission or charge. Provided that the authors, title and full bibliographic details are credited, a hyperlink and/or URL is given for the original metadata page and the content is not changed in any way.

---

---

---

City Research Online:

<http://openaccess.city.ac.uk/>

[publications@city.ac.uk](mailto:publications@city.ac.uk)

---

# Sustainable and Resilient Seismic Design of Reinforced Concrete Frames with Rocking Isolation on Spread Footings

Panagiotis E. Mergos <sup>a,\*</sup>

<sup>a</sup> *Department of Civil Engineering, City, University of London, London EC1V 0HB, UK*

## Abstract.

The rapidly evolving climate change together with the urgent need of modern societies for resilience against catastrophic threats set the sustainable and resilient seismic design of reinforced concrete (RC) structures as a priority. Rocking isolation of RC frames resting on spread footings has been proven numerically and experimentally to offer superior seismic performance with reduced seismic demands in the superstructure. At the same time, rocking footings do not require special construction solutions and can be readily implemented in the current state of practice. To exploit these benefits, the present study, for first time, utilizes rocking footings in the optimum design of RC frames for high seismic resilience and reduced environmental impact. This is achieved by incorporating a resilient seismic design methodology into a numerical optimization procedure that is aiming to minimize embodied carbon. Applications of the proposed approach show that the carbon footprint of RC frames can be reduced by 40% due to rocking isolation on spread footings. The benefits become more important as the level of seismic hazard increases. It is also found that the environmental benefits of rocking footings for RC frames are rather insensitive to the characteristics of ground motions and the uncertainties of soil properties.

**Keywords:** Reinforced Concrete Frames; Rocking Isolation; Spread Footings; Structural Optimization; Genetic Algorithm; Embodied Carbon

## Acknowledgments and Funding Information

No funding was received to assist with the preparation of this manuscript.

## 1 Introduction

Reinforced concrete is ubiquitous in the built environment. At the same time, it is responsible for high environmental impacts, such as greenhouse gas emissions, contributing significantly to current climate change [1]. This is mainly attributed to its two constituents: cement and reinforcing steel. Cement alone is responsible for 7% of global CO<sub>2</sub> emissions [2]. Furthermore, reinforcing steel can generate embodied carbon, measured in kgCO<sub>2e</sub>, up to approximately two times its own weight [3].

---

\* Corresponding author. Panagiotis E. Mergos, Senior Lecturer in Structural Engineering, Research Centre for Civil Engineering Structures, City, University of London, London, EC1V 0HB, UK.  
E-mail address: [panagiotis.mergos.1@city.ac.uk](mailto:panagiotis.mergos.1@city.ac.uk), Tel. 0044 (0) 207040 8417

Rigid frames are widely used in concrete buildings since they can form various structural configurations while maintaining a high degree of redundancy with multiple load paths. Furthermore, the high deformation and ductility capacity of concrete frames makes them particularly efficient in earthquake prone regions [4]. However, concrete frames are rather complex structural systems with multiple design variables and nonlinear design constraints turning their efficient structural design into a challenging computational task. To cope efficiently with this task, the use of structural optimization algorithms and methodologies is generally required [5-8]. There exists a great number of studies on the numerical structural optimization of RC frames subjected to static loads (e.g. [5, 9-11]). Furthermore, there exists a significant number of studies addressing the optimum seismic design of RC frames either with conventional force-based procedures (e.g. [12-15]) or performance-based methodologies (e.g. [16-21]).

At the same time, experience from previous catastrophic earthquakes has demonstrated the need for resilience in seismic design, that is the ability of buildings to absorb earthquakes when they occur and to recover quickly afterwards [22]. In resilient seismic design, the concept of seismic isolation plays a key role since it disconnects structures from ground shaking reducing structural forces and damage [23-25]. Despite the great advances in seismic isolation research and the development of robust isolation systems and design procedures, the application of seismic isolation solutions in real world applications is still rather limited [26-27]. This is partly due to the requirement for special construction solutions not compatible with the present state of practice.

Rocking isolation is a seismic isolation approach, where rocking and uplifting are allowed and used to limit seismic forces in structures. These response mechanisms were, most likely, the main reasons behind the observed, in previous earthquakes, excellent seismic performance of seemingly unstable structural systems, such as free-standing ancient temples, water tanks and slender bridge piers [28]. The theoretical background of the dynamic response of rocking

structures has been thoroughly investigated in more than 60 years (e.g. [28-32]) and useful conclusions have been made regarding the stability of these systems with respect to the characteristics of ground motions.

In literature, two main approaches of rocking isolation are met [33]. In the first approach, rocking columns, with or without a tendon, are designed to rock and uplift on rigid foundations (e.g. [34-36]). In the second approach, columns are monolithically connected to footings that are under-designed so that they rock and uplift on the underlying soil. The latter footings are commonly termed “rocking footings” [33,37-38]. A significant advantage of rocking footings is that they comply with current construction practice, and they don’t require special connections or additional protection measures. Furthermore, rocking footings have high resistance against overturning collapse due to their low aspect ratios [33].

Several numerical studies have compared the response of RC bridges and buildings resting on rocking footings against the conventional design approach, where footings are over-designed so that damage is guided to structural members (e.g. [33, 38-42]). It has been found consistently that rocking footings offer superior performance in reducing structural damage, preventing collapse and eliminating residual deformations thereby increasing seismic resilience. Furthermore, there now exists extensive experimental evidence to support the beneficial and robust seismic performance of rocking foundations [43].

The advantageous seismic performance of structures on rocking foundations inspired Anastasopoulos et al. [40] to introduce a new seismic design philosophy that utilises rocking foundations to protect the superstructure reversing the conventional seismic design approach. Interestingly, the authors, in their rationale for supporting this philosophy, explain that using foundations as safety-valves limits accelerations transmitted to the superstructure and this could offer economy not only in the foundation but also in the superstructure without compromising safety. In the following years, detailed displacement-based [44] and

performance-based [45] seismic design methodologies have also been proposed for bridges and buildings with rocking foundations.

In the following, a simple procedure for designing RC frames resting on rocking footings will be presented that maximizes seismic resilience and complies fully with current design guidelines, such as the Eurocodes. Next, an optimization framework is developed for minimizing the environmental impact of these structural systems for improved sustainability. The ultimate objective is to compare the minimum environmental footprint of RC frames on rocking footings against the conventional design solutions and thereby make useful conclusions regarding the sustainability benefits of the novel design approach. A simple but realistic 3D RC frame case study is designed parametrically to facilitate these comparisons.

## **2 Seismic design methodology**

### **2.1 Conceptual design**

In conventional seismic design, RC frames are designed either as dissipative or non-dissipative (or low dissipative). The former are able to dissipate energy by means of ductile hysteretic behaviour. Foundations of dissipative RC frames are designed on the basis of capacity design principles so that they remain undamaged even after the development of potential over-strengths at the column bases. Superstructures and foundations of non-dissipative RC frames are designed elastically.

In the proposed approach, foundations are under-designed so that they exhibit rocking and uplifting response, that acts as mechanical fuse for the seismic forces in the superstructure, and the superstructure is designed to remain elastic or with minor damage. Hence, for the purposes of structural design of the superstructure, rocking isolation is treated here in a way similar to base isolation in existing design codes. More particularly, in the present study, the superstructure is designed according to Eurocode 8 (EC8) – Part 1 [46] for base-isolated RC

frames. Therein, superstructures of buildings with base isolation must satisfy the Damage Limitation (DL) and the Ultimate (ULS) limit states. At the DL limit state, inter-storey drifts of buildings should remain below threshold values, based on the type of non-structural components, under a frequent earthquake. At the ULS, the isolation mechanism may attain its ultimate capacity, while the superstructure remains nearly elastic. This is achieved by designing the superstructure according to ductility class low (DCL) for seismic forces accounting for the effects of base isolation and divided by a behaviour (force reduction) factor not greater than 1.5. Following this approach, there is no need for additional capacity design provisions and special detailing rules for local ductility in the superstructure. To account for the special characteristics in the response of rocking footings, seismic action effects are calculated herein by the use of nonlinear response history analysis (NLRHA) with appropriate considerations for both geometric (i.e. foundation uplift and P-delta effects) and material nonlinearities in the underlying soil.

Moreover, for the seismic design methodology to be complete, excessive damage in the foundation and underlying soil should be avoided. For example, Anastasopoulos et al. [40] observed that mobilization of the bearing capacity of a rocking shallow foundation may lead to significant permanent settlements that could undermine resilience of the structure. It is, therefore, important that appropriate performance criteria are set for rocking foundations. Based on experimental tests, Kutter et al. [37] suggest uplift and residual settlement as the most appropriate measures to assess performance of rocking foundations. Clearly, the performance criteria of rocking foundations should be compatible with the performance levels and target objectives of the superstructure so that the foundation does not compromise the resilience of the structure as a whole.

The proposed approach is readily implementable in current design practice in a manner similar to base isolation. Its main advantage is that it maximizes resilience by ensuring elastic response

of the superstructure. However, this comes at a price of additional upfront material costs and environmental impacts. The alternative is to allow damage in the superstructure by adopting a performance-based design framework [45]. The latter approach, however, reduces seismic resilience and increases retrofit costs and environmental impacts. Therefore, both approaches should remain available for the designers to decide based on preferences, objectives and the structure under consideration.

## 2.2 Design optimization

The afore-described design approach necessitates a prior knowledge of footing dimensions and cross-sections of the RC frames. Then, NLRHA is conducted to calculate seismic action effects on the superstructure and the foundation. Next, the superstructure inter-storey drifts should be checked against the DL limit state. Furthermore, the RC frame must be designed for low ductility to satisfy the ULS. Finally, the performance of the foundations should be examined against the corresponding acceptance criteria.

Therefore, the suggested methodology requires by the designer a pre-selection of footing dimensions and RC frames cross-sections based on experience or completely arbitrarily. However, this selection by no means guarantees maximum structural and material efficiency. This is especially the case if we consider the nonlinear structural behaviour of the RC frames resting on rocking footings, which makes their response difficult to predict. Instead, an automated structural optimization solution procedure is recommended herein for this design problem. The goal of the optimization procedure is to select the best combination of footing sizes and cross-sections of the RC frames that will satisfy all safety and serviceability requirements and at the same time minimize embodied environmental impact.

Following this approach, the seismic design of RC frames on rocking footings is set as a single-objective optimization problem, as below:

$$\begin{aligned}
&\text{Minimize:} && f(\mathbf{x}) \\
&\text{Subject to:} && g_j(\mathbf{x}) \leq 0, \quad j = 1 \text{ to } m \tag{1}
\end{aligned}$$

Where:

$$\begin{aligned}
&\mathbf{x} = (x_1, x_2, \dots, x_d) \\
&x_i \in \mathbf{D}_i = \{1, 2, \dots, t, \dots, k_i\}, \quad i = 1 \text{ to } d
\end{aligned}$$

In Eq. (1),  $f(\mathbf{x})$  is the objective function to be minimized and  $\mathbf{x}$  is the design variables vector consisting of  $d$  independent variables  $x_i$  ( $i = 1$  to  $d$ ). The variables  $x_i$  assume values from integer sets of values  $\mathbf{D}_i = \{1, 2, \dots, t, \dots, k_i\}$ , where  $t = 1$  to  $k_i$  is the  $t$ -th possible integer value of design variable  $x_i$  and  $k_i$  is the total number of possible integer values of  $x_i$ . Moreover, the design problem is subject to  $m$  constraints  $g_j(\mathbf{x}) \leq 0$  ( $j = 1$  to  $m$ ). In the following, the various components of the optimization problem of Eq. (1) are discussed in more detail.

A sizing optimization problem is adopted in this study, where concrete frame geometry, material properties and loadings are assumed fixed (i.e. design parameters). Therefore, the design variables  $x_i$  ( $i = 1$  to  $d$ ) of the optimization problem represent only cross-sections of structural members or sizes of concrete footings. For construction simplicity, structural members and footings may be included in groups of the same cross-sections and footing sizes, respectively. In this case, design variables represent the common cross-sections or footing sizes of the corresponding groups (i.e. one design variable per group). The design variables  $x_i$  take values from integer values sets  $\mathbf{D}_i = \{1, 2, \dots, t, \dots, k_i\}$ , reflecting the positions of cross-sections or footing dimensions in corresponding lists of available cross-sections and footing dimensions, and  $k_i$  is the total number of available cross-sections or footing dimensions in the list of  $x_i$  ( $i = 1$  to  $d$ ). For simplicity in this study, lists of available square cross-sections are assumed for concrete columns and rectangular sections for beams with general configuration and steel reinforcement, as shown in Fig. 1.

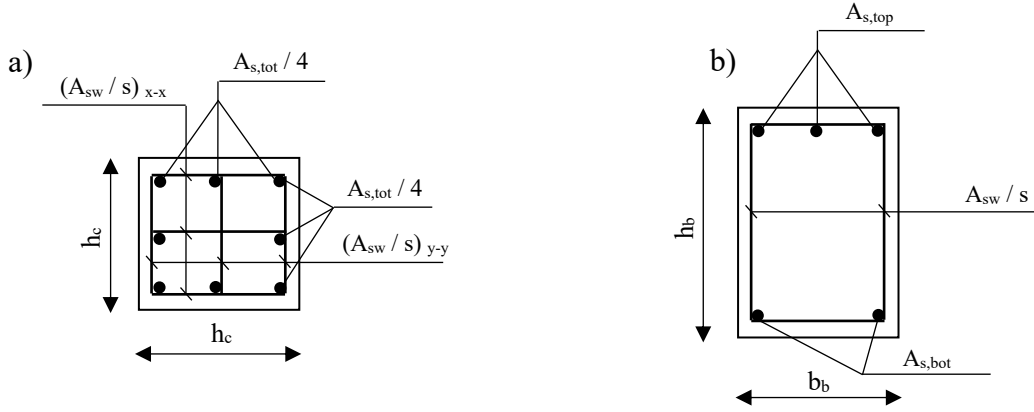


**Fig. 1:** Cross-sectional characteristics: a) column sections; b) beam sections

For a given design vector  $\mathbf{x}$  (i.e. set of RC frame cross-sections and footing sizes), NLRHA is used to calculate internal forces in the superstructure accounting for rocking isolation effects. Then, the structural members of the RC frames are designed for strength, to calculate their required steel reinforcement, according to the provisions of DC Low in EC8. More specifically, concrete beams are designed for major bending to establish the required longitudinal reinforcement and major shear with torsion to calculate the required transverse reinforcement. Concrete columns are designed for biaxial bending with axial load to calculate the required longitudinal reinforcement. Furthermore, the required shear reinforcement is calculated in both horizontal directions for the corresponding shear forces. More details regarding the calculation of steel reinforcement in the concrete frames can be found in [13-14].

Having established the concrete sections and steel reinforcement, the objective function  $f(\mathbf{x})$  is calculated. In the present study, the objective function is set to be the environmental footprint of the RC frames and foundations in terms of embodied carbon ( $\text{kgCO}_2\text{e}$ ). It is emphasized that the embodied carbon of other structural components, such as RC slabs, should be considered in the total structural carbon of RC buildings. However, the current study focuses solely on the environmental impact of the structural systems that are expected to be significantly influenced by rocking isolation in the context of seismic design.

The embodied carbon is calculated as the sum of contributions of concrete and reinforcing steel. The latter includes both the transverse and longitudinal steel reinforcement. More particularly, Eq. (2) is used to calculate embodied carbon, where  $V_c$  ( $m^3$ ) and  $m_s$  (kg) is the total concrete volume and steel mass, respectively, of the RC frames and foundations and  $f_{co}$ , and  $f_{so}$  are the corresponding embodied carbon coefficients of concrete and reinforcing steel materials. The recommendations in Kaethner and Burrige [47], for the typical environmental impact scenario, are adopted in this study for the material carbon coefficients. The latter coefficients refer to cradle to gate embodied CO<sub>2</sub> emissions that address both raw material extraction and factory production processes [47].

$$f(\mathbf{x}) = V_c(\mathbf{x}) \cdot f_{co} + m_s(\mathbf{x}) \cdot f_{so} \quad (2)$$

For a design solution to be feasible, all design constraints  $g_j(\mathbf{x}) \leq 0$  ( $j = 1$  to  $m$ ) should be satisfied. In the problem under consideration, inter-storey drifts for the frequent earthquake should remain below the DL Limit state values as specified in EC8-Part 1. Furthermore, the performance of footings should be checked against appropriate deformation-based acceptance criteria [37]. In both cases, the design constraints can be written in the following form, where  $EDP$  is the corresponding engineering (deformation) demand parameter and  $EDP_{lim}$  is the respective threshold value for the Limit State under examination.

$$EDP - EDP_{lim} \leq 0 \quad (3)$$

In addition to the performance constraints, the constraints of the non-dissipative design of the superstructure must be considered. A design is not acceptable in this case, when the required longitudinal  $\rho_l$  and transverse  $\rho_w$  reinforcement volumetric ratios, in even one of the design

cross-sections of the RC frame, exceed their maximum permissible values as specified by the design codes and construction practice. The corresponding constraints are written as:

$$\rho_l - \rho_{l,max} \leq 0 \quad (4)$$

$$\rho_w - \rho_{w,max} \leq 0 \quad (5)$$

Furthermore, to prevent diagonal compression failure, the RC frame cross-sections should satisfy the following constraint, where  $V_{Ed}$  and  $T_{Ed}$  are the shear force and torsional moment demands, respectively, and  $V_{Rd,max}$  and  $T_{Rd,max}$  are the corresponding diagonal compression capacities for an angle of compression struts  $\theta = 45^\circ$ .

$$\frac{V_{Ed}}{V_{Rd,max}} + \frac{T_{Ed}}{T_{Rd,max}} - 1 \leq 0 \quad (6)$$

The proposed optimization methodology is summarized in Fig. 2. It is noted that when the design constraints are not satisfied then the design solutions are branded as unfeasible, the analysis is terminated, and a large “penalty” value is added to their objective function that exceeds greatly expected environmental costs. In this context and to reduce computational cost, the design constraints are checked gradually to avoid unnecessary and computationally expensive structural analysis and design procedures.

An efficient optimization algorithm (optimizer) is required to solve the afore-described optimization problem. The challenge of the optimization algorithm is to identify the global optimum solution without getting trapped in local optima and with the minimum possible number of numerical iterations. The latter is particularly important in the problem under investigation, where the required nonlinear response history analyses increase sharply the computational burden. A thorough discussion and comparison of various algorithms in the optimum design of RC frames can be found in [13-14]. A mixed-integer Genetic Algorithm

(GA) [48-49] is adopted in this study that offers a good combination of search space exploration and exploitation capabilities [13-14].

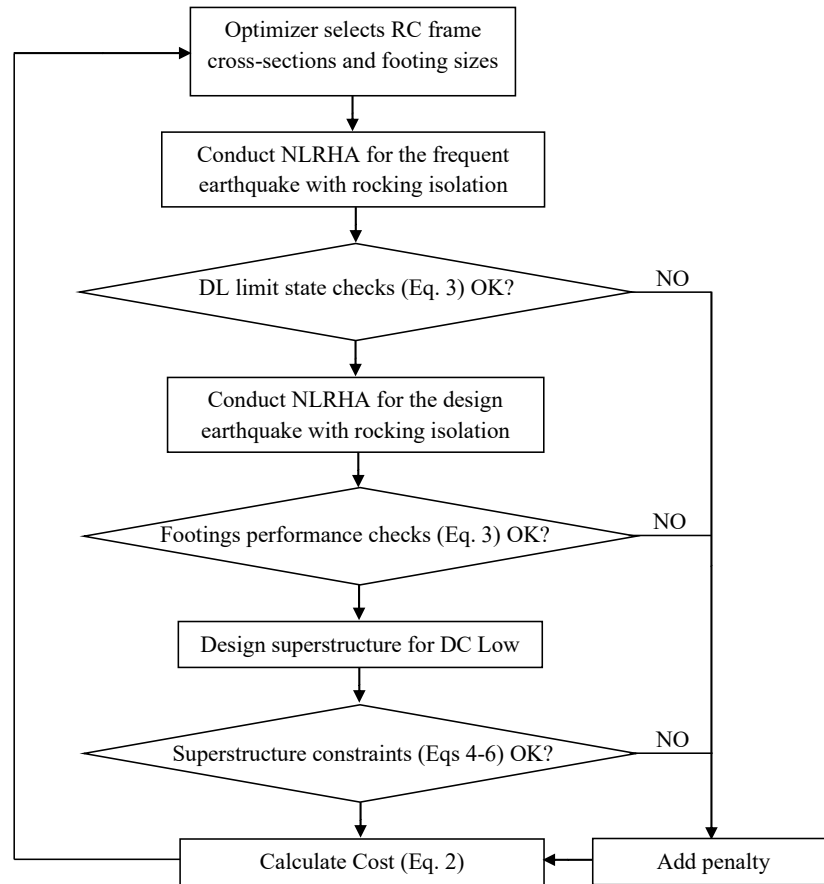


**Fig. 2:** Optimum seismic design methodology

### 3 Design implementation

#### 3.1 RC frame design case-study

In this section, a three-storey, symmetric, 3D portal building RC frame is examined with span length of 6m and storey height of 3m (Fig. 3). Concrete class C25/30 and reinforcing steel class B500C are used following the specifications of Eurocode 2 (EC2) [50]. Due to symmetry, one cross-section is used for all corner columns and one cross-section for all the perimeter beams of each storey. Therefore, four independent concrete cross-sections are assumed for this frame (i.e.  $d = 4$  in Eq. 1). Based on a preliminary analysis, a list of six available rectangular

cross-sections is considered for concrete beams and of eleven square cross-sections for concrete columns, as shown in Table 1. Following these considerations, the size of the search space for the optimization problem of Eq. (1) is  $11 \cdot 6^3 = 2376$  possible RC frame cross-section configurations. All cross-sections are assumed to have the general forms of Fig. 1. Furthermore, concrete cover to the centroid of the longitudinal steel bars is taken as 50mm.

**Table 1:** Lists of available frame cross-sections

RC beams sections $b_b \times h_b$	(0.25x0.25; 0.25x0.30; 0.25x0.35; 0.25x0.40; 0.25x0.45; 0.25x0.50)
RC columns sections $h_c \times h_c$	(0.25x0.25; 0.30x0.30; 0.35x0.35; 0.40x0.40; 0.45x0.45; 0.50x0.50; 0.55x0.55; 0.60x0.60; 0.65x0.65; 0.70x0.70; 0.75x0.75)

The concrete building is designed to withstand static and seismic loads. For static loads, the building is designed in accordance with EC2. Slab dead loads are taken as  $8.25 \text{ kN/m}^2$  (inclusive of self-weight) for all storeys apart from the top storey where they become  $10.25 \text{ kN/m}^2$  because of the existence of a roof garden. Slab live loads are  $5 \text{ kN/m}^2$  for all storeys. Moreover, the concrete building is designed against earthquake loads following EC8 and in accordance with the methodology described in the previous sections. The building is in a high seismicity region and therefore the EC8 Type 1 response spectrum is considered to represent seismic action. The design acceleration on rock  $a_g$  is taken equal to  $0.56g$ , that is the product of a reference peak ground acceleration  $a_{gR} = 0.40g$  by the importance factor  $\gamma_I = 1.40$ , assumed here because the integrity of this building is of vital importance for civil protection. The behaviour factor  $q$  is taken equal to unity for fully elastic response of the superstructure. Furthermore, to satisfy the damage limitation (DL) prescriptions of EC8, it is specified that inter-storey drifts should remain below 1% for the frequent earthquake. The latter threshold assumes non-structural elements fixed in a way that they do not interfere with structural deformations. The frequent earthquake is assumed to have a design ground acceleration that is equal to 40% of the reference seismic action. The building rests on gravel having  $N_{SPT}$  value

over 50. Modulus of subgrade reaction  $k_{sv}$  (kN/m<sup>3</sup>) is  $10^5$  and yield strength of the underlying soil is 6 MPa. For the purposes of seismic design, this soil is classified as Ground Type B in EC8.

Seismic actions are represented by artificial accelerograms generated to match the elastic response spectrum of EC8 for the input given above. The motions were generated from real accelerograms recorded on soil type B following spectral matching in the time domain as implemented in [51]. More particularly, three pairs of horizontal ground motion records were considered. The most onerous results, of the three ground motions pairs, are used in the final designs following the requirements of EC8. Fig. 4 shows the spectra of all six artificial ground motion records together with the smooth EC8 spectrum represented by the thick and continuous black line. All spectra in Fig. 4 are normalized to  $a_g \cdot S$ , where  $S$  is the soil amplification factor taken as 1.2 for Soil B in EC8.

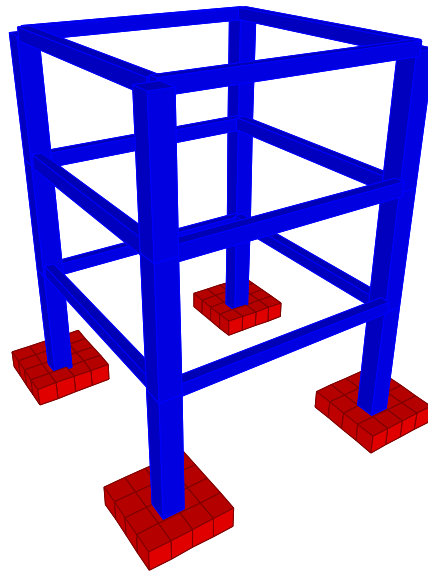


**Fig. 3:** RC frame case-study

From a preliminary response spectrum analysis of the RC frame assumed fixed at the base, it is found that to conventionally limit eccentricity below one third of the footing dimension, the sizes of the isolated footings should be so large that practically a foundation slab solution is

required. Instead, the use of square rocking footings is adopted herein with width of 2m. A parametric study later also reveals the effect of various footing sizes on the optimal design of the RC frame. It is also noted that, for all the footing sizes considered, no yielding of the underlying soil was detected and therefore the performance of the footings does not compromise the design of the RC frames.

In the present study, soil-structure interaction is modelled by a 2D mesh of distributed and independent, compression-only (i.e. zero stiffness in tension), soil springs (i.e. Winkler model), as shown in Fig. 5. This approach directly considers foundation uplift and accounts explicitly for the interaction between axial load and biaxial bending moment capacity of the rocking footings. It is interesting to note that, for a number of simplifying assumptions (i.e. uniaxial and monotonic loading, constant vertical load, small deformations, rigid footings and linear elastic soil response), the afore-described modelling approach yields Eq. (7) relating the bending moment  $M_f$  and the corresponding rotation  $\theta_f$  at the base of the footing before foundation uplift and Eq. (8) for the response after foundation uplift. The latter initiates at

$$M_f = \frac{N_f L_f}{6}.$$

$$M_f = \frac{k_{sv} B_f L_f^3}{12} \theta_f \quad (7)$$

$$M_f = N_f \cdot \left( \frac{L_f}{2} - \frac{1}{3} \sqrt{\frac{2N_f}{k_{sv} B_f \theta_f}} \right) \quad (8)$$

In these equations,  $L_f$  is the footing dimension in the plane of  $M_f$ ,  $B_f$  is the footing dimension out of the plane of  $M_f$  and  $N_f$  is the vertical load at the base of the footing. Eqs (7-8) are useful for understanding the controlling parameters in the response of rocking footings before and after foundation uplift. However, they cannot reliably replace the 2D mesh of springs used herein in the realistic seismic analysis of RC frames resting on rocking footings.

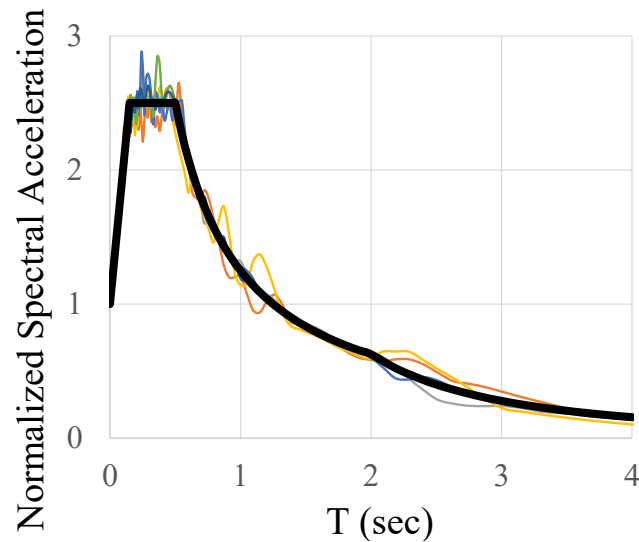


**Fig. 4:** Response spectra

Static and seismic (NLRHA) structural analyses were conducted with the aid of computer software SAP2000 [52]. A direct integration of the equation of motion numerical procedure was followed using Newmark's method with  $\gamma = 0.5$  and  $\beta = 0.25$  (i.e. average acceleration method). Direct integration is sensitive to the size of the time step. Following a preliminary analysis, a NLRHA time step of 0.005s was found adequate for the purposes of this study. The modified Newton-Raphson method is used to account for the nonlinearities stemming from foundation uplift and P-delta effects. Flexural stiffness of the concrete structural members is reduced to 50% of the uncracked, following the recommendations of EC8. Furthermore, P-delta effects were duly taken into account in all seismic analyses. Structural design of the RC frame, for the calculation of required steel reinforcement and design constraints according to the Eurocodes, is also conducted with the aid of SAP2000 for the static load combination  $1.35G+1.5Q$  and the seismic load combination  $G+0.3Q\pm E$ , where G, Q and E represent permanent, live and earthquake actions respectively. A MATLAB [53] application developed by the author, namely STROLAB [13], interacts with SAP2000, via its API, for the purposes of structural optimization.

For simplicity in the calculation of the objective function, it is assumed that the provided steel reinforcement areas match the required ones, as calculated by SAP2000. Furthermore, only

the environmental impact of the RC frame is considered in the calculations so that the study focuses on the benefits of rocking footings to the superstructure. However, the rather obvious reduction, with respect to conventional foundation design, of foundation's environmental footprint with the adoption of rocking footings should also be accounted when selecting the most appropriate design approach. In the calculations of environmental footprint, the embodied carbon coefficient used for concrete is  $f_{co} = 228 \text{ kgCO}_2\text{e}/\text{m}^3$  and for reinforcing steel  $f_{so} = 0.87 \text{ kgCO}_2\text{e}/\text{kg}$ , respectively [47]. In the following, the RC frame is optimally designed either as fixed at the base or with rocking footings to compare the conventional and suggested seismic design approaches.

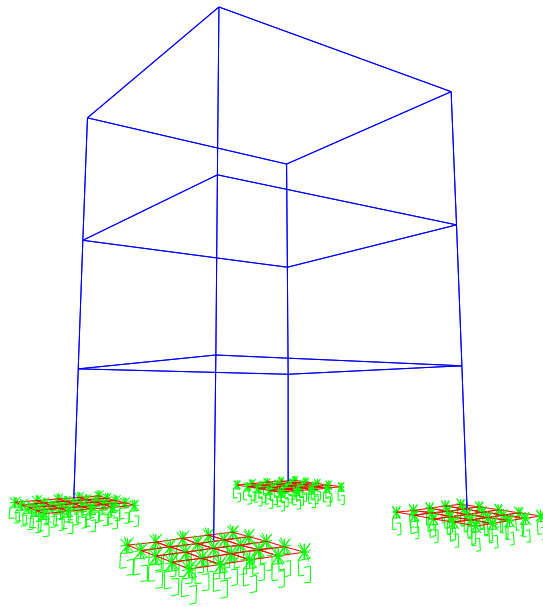


Fig. 5: Modelling of rocking footings

### 3.2 Optimization analysis

The optimization analysis assumed in this study requires the use of a numerical optimization algorithm to track the design solutions that minimize environmental footprint of RC frames. Exhaustive search (ES) is such an algorithm that examines all possible combinations of design variables and tracks the one with minimum cost. ES requires high computational costs, but it

guarantees tracking of the global optimum solution. In the specific case-study, ES requires all 2376 possible RC frame cross-sectional configurations to be designed following a number of nonlinear response history analyses for each configuration. This was judged not practical for the purposes of this study that will examine parametrically several optimal designs of the RC frame.

Following the previous considerations, a mixed-integer GA is used herein that combines well global and local search capabilities. However, the GA, and all evolutionary optimization algorithms, are not guaranteed to track global optima. Hence, to validate the efficiency of the GA in the problem under investigation, an ES analysis is first conducted for the designs of the RC frame assuming only one set of ground motions (i.e. for reduced computational cost). Fig. 6a presents the embodied carbon of all ES design solutions (ranging from 1 to 2376), for one set of horizontal ground motions, assuming the frame either as fixed or with rocking footings. Only feasible design solutions are shown. Generally, in this figure, as the solution number increases the size of RC frame cross-sections increases. It is seen that the embodied carbon of the designs with rocking footings is significantly lower (i.e. in the order of 20%) than the carbon of the fixed frames for the same design solutions (i.e. same RC frame cross-sections). This is a clear indication of the rocking isolation effect that reduces seismic actions effects in the frame and thereby steel reinforcement requirements. Importantly, this rocking isolation effect seems to work for all RC frame cross-sections combinations, which shows its robustness in mitigating seismic action effects. It is also noted that the number of feasible solutions greatly increases in the case of rocking foundations. This is again justified by the reduced action effects that make designs with smaller cross-sections to satisfy all design constraints. As a result, the minimum embodied carbon of all design solutions is 6316 kgCO<sub>2</sub>e for the frame on rocking footings as opposed to 9620 kgCO<sub>2</sub>e for the fixed frame (i.e. 34% reduction)

Fig. 6b, demonstrates the relationship between total concrete volume  $V_c$  versus total reinforcing steel mass  $m_s$  for the same feasible ES solutions. The Pareto fronts of these

solutions are also presented. It is clear that the designs of the fixed frame require significantly more steel reinforcement for the same concrete volume of the rocking frame. It is also evident that design solutions with significantly less concrete are feasible when rocking footings are used.

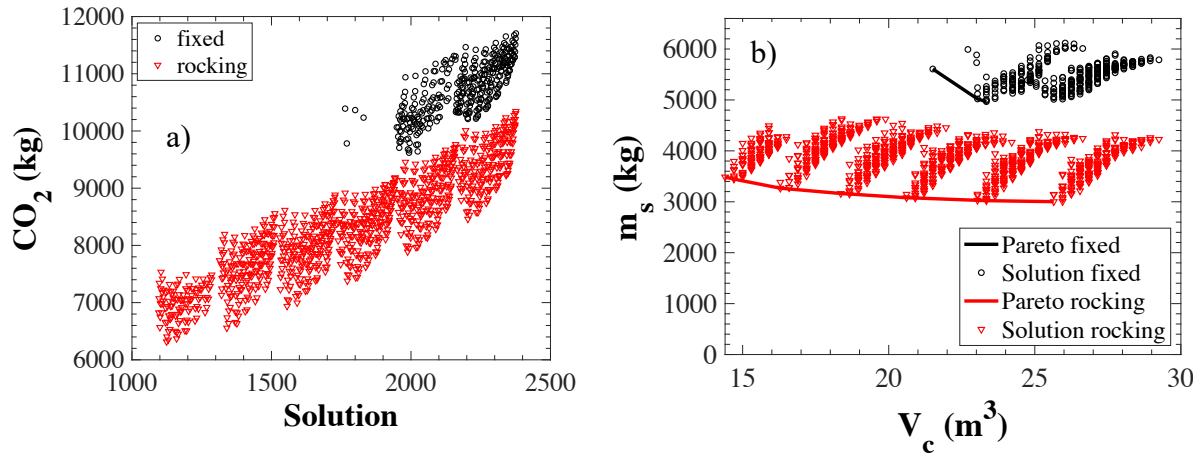


**Fig. 6:** Exhaustive analysis results for one set of ground motions

To investigate the validity of the GA algorithm, 10 independent GA runs are conducted for the fixed and rocking frame with the same assumptions as the previous ES. It is found that, in all cases, the GA returns the same optimum solutions within 300 evaluations (i.e. trial design solutions), as shown in the two example runs in Fig. 7. In this figure, the markers represent the carbon of the current evaluations and the solid lines the current best design solutions with the number of function evaluations. Therefore, the GA algorithm is used for the optimum designs in the rest of this study with 300 function evaluations (i.e. almost 8 times fewer than ES).

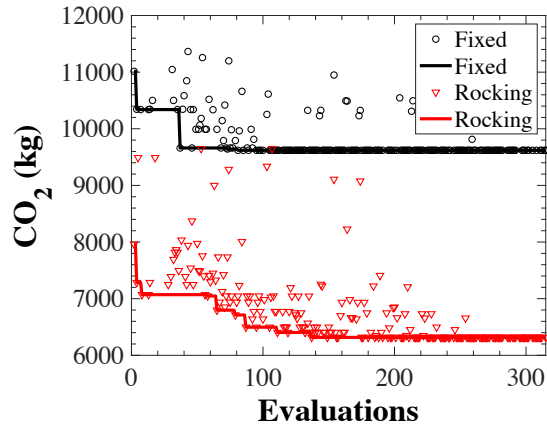


**Fig. 7:** Example GA run histories used for algorithm validation

### 3.3 Optimal design solutions

With the GA settings of the previous section, the RC frames are designed optimally considering the worst results of all three pairs of ground motions, as required by EC8. Fig. 8a, shows the GA convergence histories and Fig. 8b the obtained minimum embodied carbon for the fixed and rocking frame, which are 11599 kgCO<sub>2e</sub> and 6994 kgCO<sub>2e</sub> respectively. Therefore, a 40% reduction in the embodied carbon was achieved by the use of rocking footings with respect to the conventional design. The values reported here are slightly larger than the ones discussed in §3.2 since three ground motion pairs are applied instead of one. The sections of the optimal design solutions are given in Table 2. It is evident that the two optimal frames have very different cross-sections with the fixed frame requiring significantly larger concrete sections. This is better illustrated in Fig. 9 comparing the 3D geometries of the two frames with concrete sections presented in the same scale.

**Table 2:** Optimal design solutions cross-sections

RC frame group of members	Optimal cross-section	
	Frame on Rocking Footings	Fixed Frame
<b>Corner Columns</b>	0.50X0.50	0.75X0.75
<b>Beams 1<sup>st</sup> floor</b>	0.25x0.30	0.25x0.50
<b>Beams 2<sup>nd</sup> floor</b>	0.25x0.35	0.25x0.30
<b>Beams 3<sup>rd</sup> floor</b>	0.25x0.30	0.25x0.30

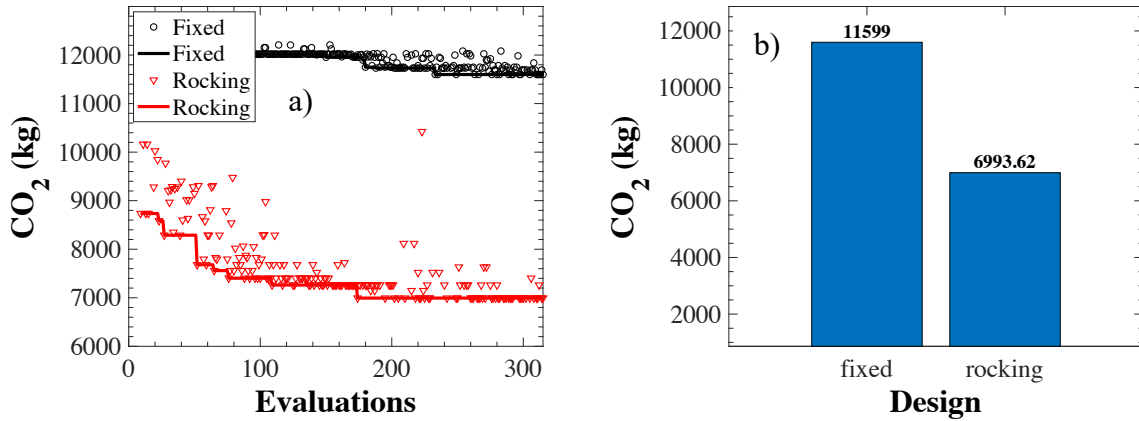


**Fig. 8:** Optimal design solutions: a) GA runs; b) minimum embodied carbon

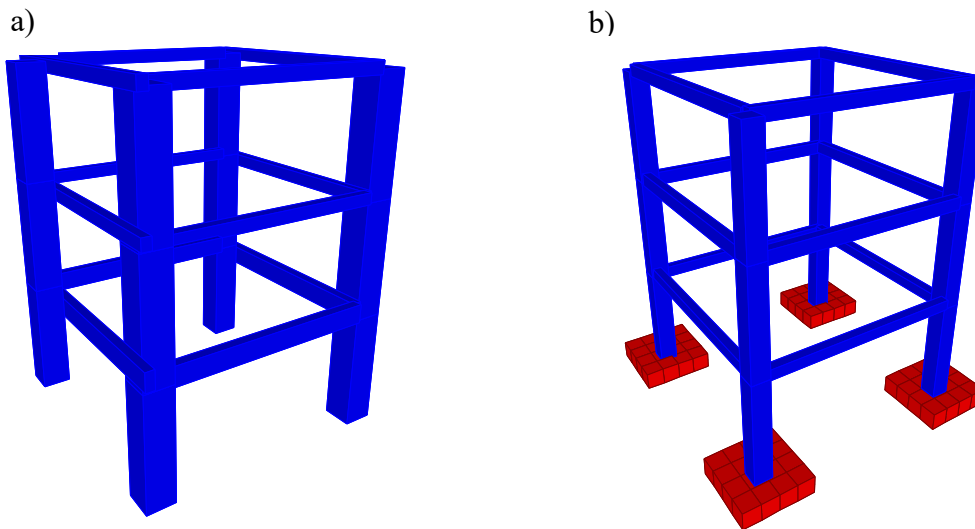
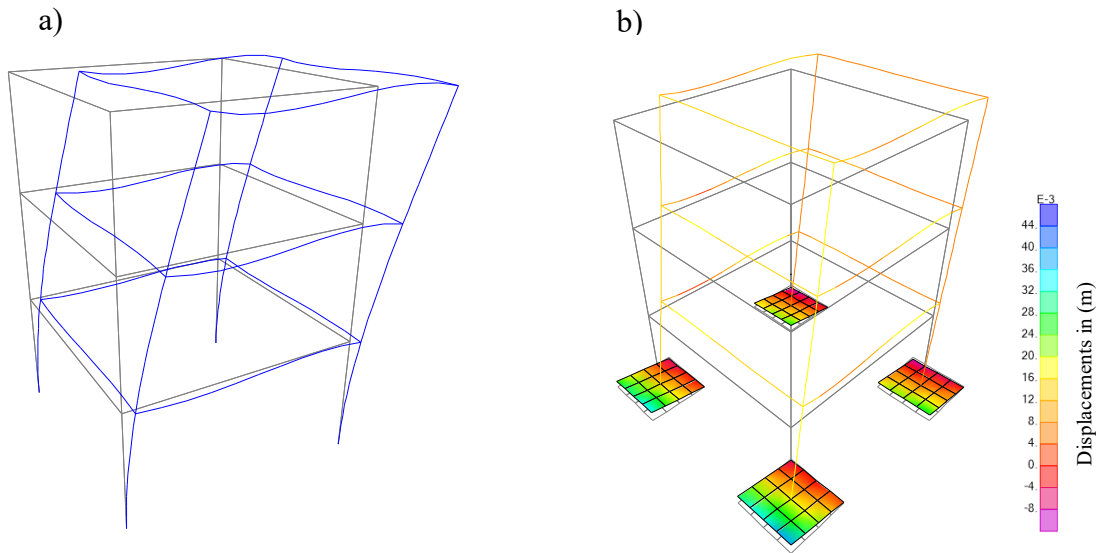


**Fig. 9:** Optimal design solutions: a) Fixed frame; b) frame on rocking footings

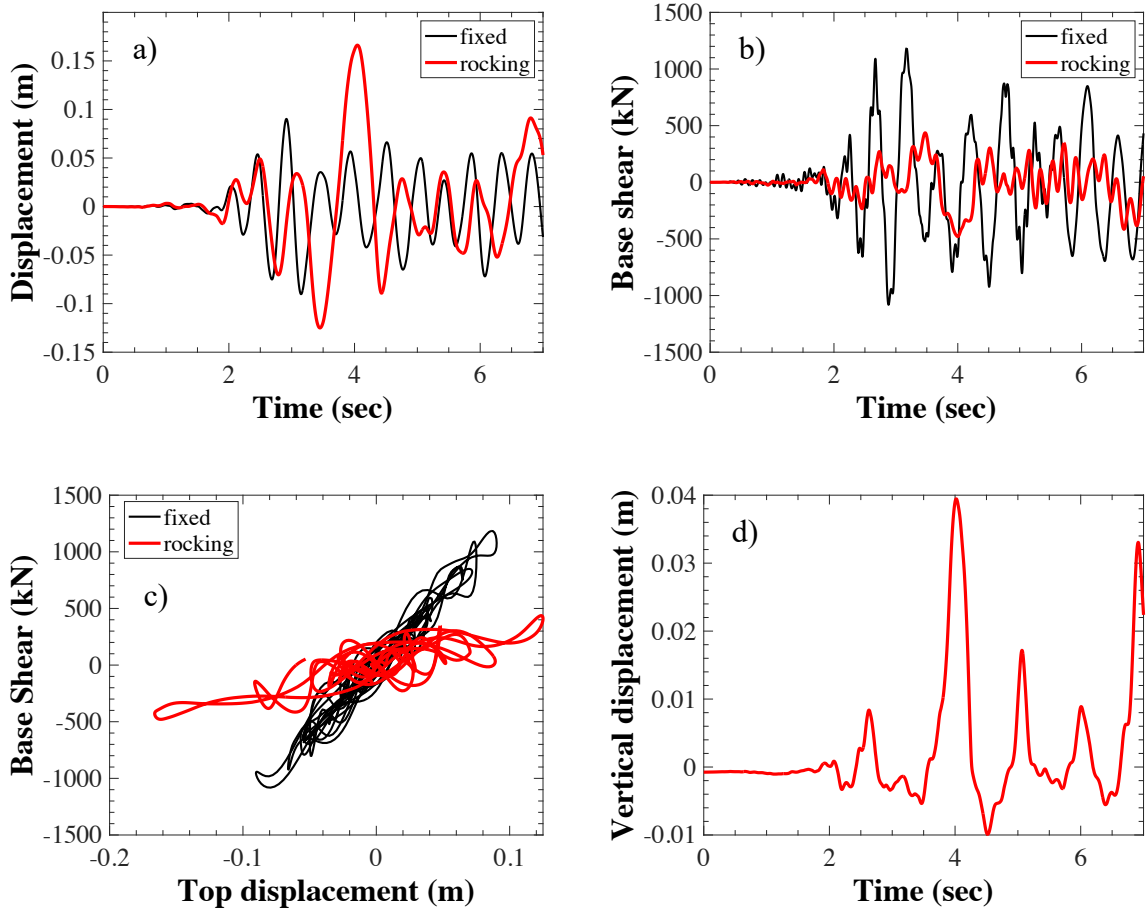
Furthermore, Fig. 10 presents the deflection responses, at the instance of maximum deflection in one horizontal direction for one pair of ground motions, of the two optimal RC frames. From the displacement contour plot in Fig. 10b, it is evident that footings uplift in more than half of their area, which proves the extent of rocking response. It is also clear that the rocking response is generating significant rotations at the column bases as opposed to the fixed frame.

Furthermore, Fig. 11 demonstrates the detailed responses of the optimal RC frames in one horizontal direction and for one pair of ground motions. More specifically, Fig. 11a compares the top displacement responses of the optimal fixed frame and the optimal frame with rocking isolation. It is important to remember here that these frames have different cross-sections, as

shown in Table 2. It is evident that displacements are significantly higher in the frame with rocking footings (0.17m instead of 0.09m), but still not prohibitive. It is also apparent that the rocking frame is more flexible than the fixed one. This is due to both the rocking response and the fact that smaller cross-sections are required for the rocking frame. The increase in lateral displacements and flexibility due to rocking response should always be treated with concern as it could cause significant non-structural damages and overturning collapse. Hence, it is important that lateral displacements are appropriately controlled (see Eq. 3) and nonlinear P-delta effects are duly taken into account in seismic analysis. Figure 11b, presenting the base-shear response of the RC frames, demonstrates that the maximum base shear drops by almost 60%, from 1182kN to 478kN, with the use of rocking foundations. This significant reduction is due to a virtuous circle effect in the optimum design with rocking footings. First, rocking isolation restricts transmission of seismic forces to the superstructure. Second, the reduced seismic action effects in the superstructure lead to smaller cross-sections for the optimal RC frame. The latter increases the period of vibration and reduces the elastic base shear in the frame for flexible systems, as shown in Fig. 4. For the two RC frames of Table 2, for example, the fundamental period of vibration increases from 0.55s, for the optimal fixed frame, to 0.95s for the optimal frame on rocking footings. In addition, for the RC frames on rocking footings, foundation uplift leads to softening of the seismic response driving to further reductions in seismic demands. Figure 11c shows the base-shear versus top displacement responses of the two RC frames. This figure clearly shows the isolation effect of rocking footings. It is seen that the rocking frame develops a “yield-like” response with a maximum base shear restricted by the moment capacity of the rocking footings.



**Fig. 10:** Deflections at maximum response in one direction of the optimal: a) fixed frame; b) frame on rocking footings



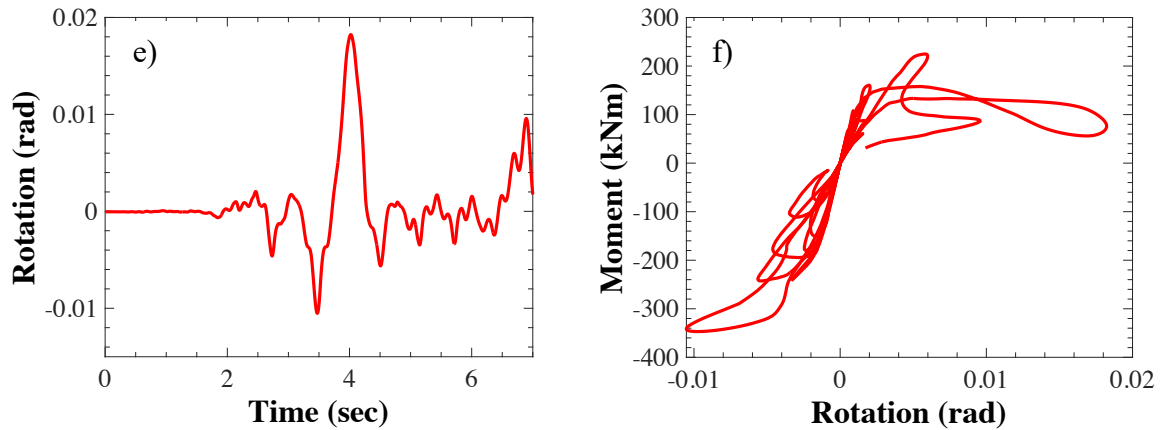


**Fig. 11:** Seismic responses of RC frames shown in Table 2: a) top displacement time-histories; b) base-shear time histories; c) top displacement versus base-shear; d) vertical displacement response at the corner of a rocking footing; e) rotation response at the base of a column resting on rocking footings; f) moment versus rotation response at the base of a column resting on rocking footings

Figure 11d presents the vertical displacement time-history of a rocking footing corner point. It is seen that the footing uplifts significantly, up to 0.04m, whereas the maximum settlement is only 0.01m. Furthermore, Fig. 11e shows the rotation response at the base of a column due to rocking of the footing below. It is found that the footing develops significant rotations up to approximately 0.018 rad. Considering that the total building height is 9m and that the maximum displacement at the top (see Fig. 11a) is 0.17m, it is concluded that rocking fully dominates the maximum lateral response of the frame. Finally, Fig. 11f presents the base moment versus base rotation of the same column as Fig. 11e. The “yielding-like” behavior due to rocking isolation is again evident.

### 3.4 Parametric optimum designs

To generalize the conclusions of the previous section, an extensive parametric study is conducted herein to investigate the effects of various design parameters such as the peak ground acceleration, characteristics of ground motions, modulus of subgrade reaction and the size of rocking footings on the optimal design of the RC frame.

### 3.4.1 The design $a_{gR}$

In this section, the RC frames of §3.1 are optimally designed for reference ground accelerations  $a_{gR} = 0.20g$  and  $0.30g$  in addition to the designs for  $a_{gR} = 0.40g$  of the previous section. Fig. 12 presents the minimum embodied carbon obtained of the fixed and rocking frames as a function of the design  $a_{gR}$ . As expected, all environmental costs increase with  $a_{gR}$ . It is also important to note that the frames on rocking footings produced always less CO<sub>2</sub> than the fixed ones. However, the difference between the two designs is rather small for low  $a_{gR}$  values (i.e.  $a_{gR} = 0.20g$ ) and becomes more important as the design  $a_{gR}$  increases. This is clearly due to the isolation effect of rocking footings limiting the seismic actions transmitted to the superstructure. This essentially means that the environmental savings due to rocking footings become more pronounced in regions of high seismicity. This conclusion is significant considering that the environmental footprint of seismic design is more important in these regions.

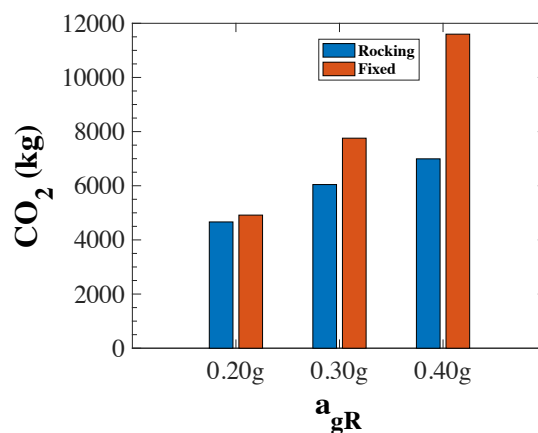


**Fig. 12:** Minimum embodied carbon of RC frames as a function of  $a_{gR}$

### 3.4.2 Ground motions characteristics

In this section, the sensitivity of the environmental impact to the characteristics of the input ground motions is investigated. More particularly, the RC frames of §3.1 are optimally designed separately for each of the three pairs of ground motions and their environmental impact is presented in Fig. 13. The difference with §3.3 is that there the frames are optimally

designed for the worst results out of the 3 pairs of ground motions in accordance with EC8 recommendations. Fig. 13 uses box plots showing the minimum, maximum and median (red line) environmental footprint. Inside the boxes, the 25<sup>th</sup> to 75<sup>th</sup> percentiles are contained.

It is observed that in all cases, as expected, the minimum environmental footprint of the fixed frames is significantly higher than the frames on rocking footings. What is more interesting to note here is the fact that the variation of minimum embodied carbon is smaller in the case of rocking footings with respect to conventional designs. The latter shows that rocking footings not only reduce the environmental impact of RC frames, but they also do so in a more robust (i.e. less sensitive) way to the characteristics of ground motions.

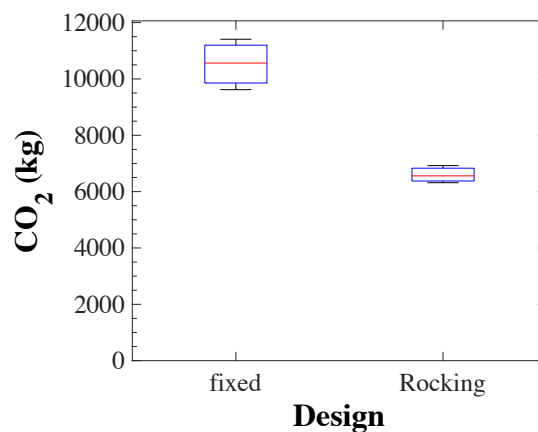


**Fig. 13:** Minimum embodied carbon of RC frames for different pairs of ground motions

### 3.4.3 Modulus of subgrade reaction

When designing with rocking footings, soil properties and modelling play an important role. In the previous, a modulus of subgrade reaction of  $k_{sv} = 10^5$  (kN/m<sup>3</sup>) was assumed. It is true that this soil property may be characterised by significant uncertainty. To investigate the influence of  $k_{sv}$  uncertainty on the optimal design of RC frames, a parametric study is conducted herein, where three significantly different values of  $k_{sv}$  are assumed (i.e.  $k_{sv} = 0.5 \cdot 10^5$ ,  $10^5$  and  $1.5 \cdot 10^5$  kN/m<sup>3</sup>) in the optimal design of the RC frames described in §3.1.

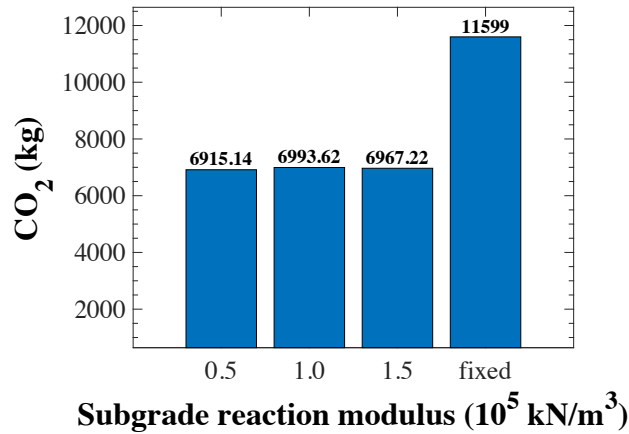
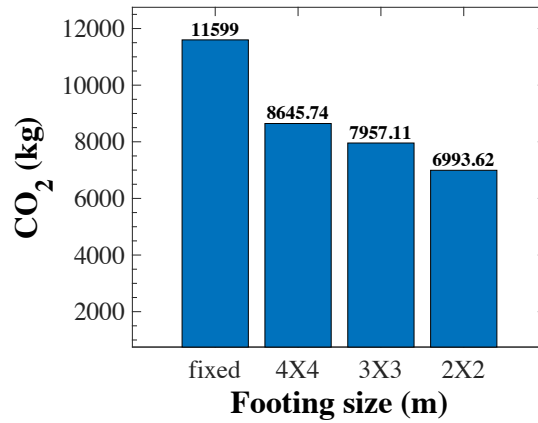


**Fig. 14:** Minimum embodied carbon of RC frames for different values of subgrade reaction modulus

Fig. 14 shows the obtained minimum environmental impacts of the fixed frame versus the frames on rocking footings for the three  $k_{sv}$  values. It is found that the minimum environmental footprint is rather insensitive to the adopted  $k_{sv}$  value for the rocking footings, within the examined range. This is important as it shows that the environmental savings, due to rocking isolation, in the optimal design of RC frames can be robust against soil uncertainties.

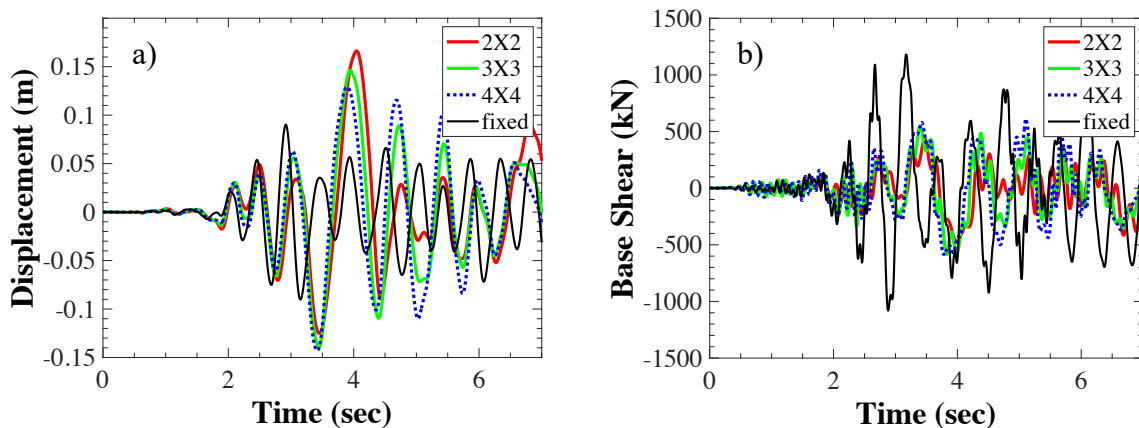
#### 3.4.4 The footing size

In section §3.1, square footings of 2m width were selected for the rocking footings. This selection led to a dominating rocking behavior for the RC frame and significant embodied carbon reductions whilst satisfying damage limitation in the superstructure and performance constraints of the foundations (i.e. no soil yielding was detected). It is more appropriate, however, that the selection of footing sizes is part of the optimization solution, as shown in Fig. 2, with the aim to minimize the combined environmental footprint of the foundation and the superstructure.



**Fig. 15:** Minimum embodied carbon of RC frames for different rocking footing sizes

In this section, to investigate the effect of footing size, the RC frame of §3.1 is designed assuming three different square footing sizes of 2m, 3m and 4m width. Figure 15 presents the obtained minimum embodied carbon for the fixed frame and the frames on rocking footings with different sizes. It is evident that the carbon footprint of the optimally designed RC frames is significantly and consistently reducing as the footing size decreases. This is explained by the fact that as the footing size reduces the moment capacity of the footing also decreases limiting the maximum seismic action effects transmitted to the superstructure. Therefore, as long as damage limitation in the superstructure and performance requirements in the foundation are satisfied, reduced footing sizes lead to reduced footprints of the superstructure.



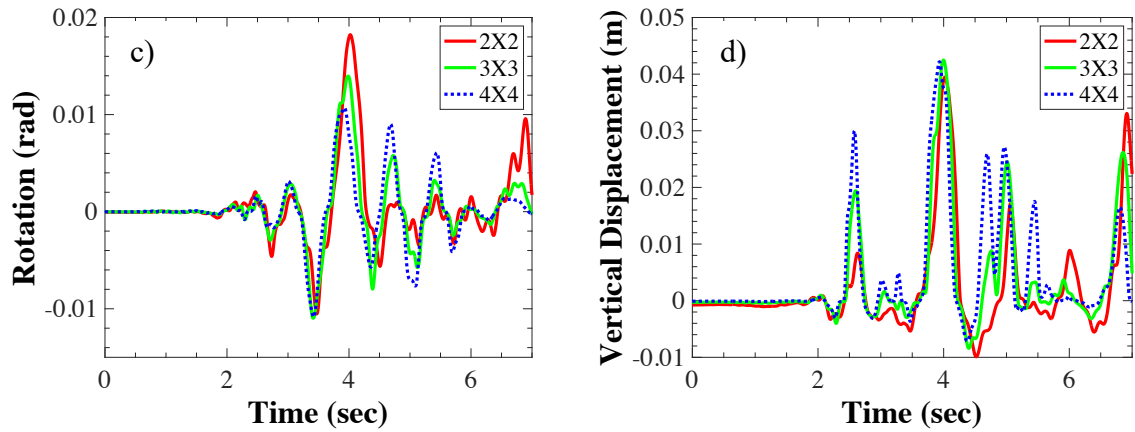


**Fig. 16:** Minimum embodied carbon of RC frames for different values of subgrade reaction modulus

Figure 16 compares seismic responses of the optimally designed RC frames with different footing sizes. Consistent findings are observed. More specifically, as the footing size increases maximum displacement decreases and base-shear force increases since RC frames become more and more fixed. This is also evident in Fig. 16c, where maximum footing rotations decrease from 0.018rad to 0.01rad as the footing width increases from 2m to 4m. Interestingly, maximum uplifts at the footing corners remain approximately the same for all footing sizes, as shown in Fig. 16d, since they represent products of footing rotations by footing dimensions. The vertical settlement is slightly decreased as the footing size increases.

## Conclusions

Current climate change requires immediate measures to reduce the environmental impact of the built environment. Furthermore, modern societies demand resilient structural systems to recover quickly after catastrophic events. In this context, the environmentally friendly and resilient seismic design of RC frames becomes a priority.

Rocking isolation of RC frames on spread footings opens a straight path in this direction since it doesn't require special construction techniques and therefore can be readily implemented in current construction practice. Furthermore, the advantageous seismic performance of RC

frames on rocking footings, with respect to conventional designs, has been extensively demonstrated by numerical studies and evidenced by experimental tests.

In this study, for first time, rocking isolation on spread footings is used to optimally design new RC frames for increased seismic resilience and reduced environmental footprint. To serve this goal, a simple seismic design methodology is suggested that accounts for the nonlinear isolation effect of rocking footings and ensures limited damage in the superstructure in addition to satisfactory foundation performance. The design methodology is complemented by a numerical optimization procedure aiming to minimize the embodied carbon of RC frames.

The proposed methodology is applied to a simple, yet realistic, 3D RC building frame of vital importance for civil protection that is located in a region of high seismicity. The RC frame is optimally designed, for minimum environmental impact, assuming rocking footings and fixed supports. It is found that the minimum possible environmental impact of RC frames on rocking footings is 40% smaller than the minimum possible footprint of conventional RC frames. It is also interesting to note that the optimal design with rocking foundations leads to significantly smaller RC frame cross sections that they wouldn't be feasible in conventional design. Even if the same cross-sections are used for the fixed and the rocking frame, a 20% reduction in the embodied carbon can be achieved by rocking footings due to the reduced requirements for steel reinforcement.

Furthermore, an extensive parametric study reveals the influence of various design parameters on the benefits of the seismic design of RC frames with rocking isolation on spread footings. It is found that the reduction of embodied carbon with rocking footings becomes more pronounced as the level of seismic hazard increases. Moreover, it is found that there is a consistent trend between reducing the size of rocking footings and saving embodied carbon in the superstructure as long as the damage limitation and foundation performance requirements are met. Finally, it seems that the environmental benefits of rocking footings are rather insensitive to the characteristics of ground motions and the uncertainties of soil properties.

## Conflict of Interest Statement

On behalf of all authors, the corresponding author states that there is no conflict of interest.

## References

1. IPCC (2021) Climate change 2021: The physical science basis. Intergovernmental Panel on Climate Change, Cambridge University Press, Cambridge, UK and New York, USA
2. IEA (2020) Energy technology perspectives 2020. International Energy Agency
3. Jones C (2019) ICE Database V3.0 Beta. Retrieved from <https://circularecology.com/embodied-energy-and-carbon-footprint-database.html>
4. Fardis MN (2009) Seismic design, assessment and retrofitting of concrete buildings. Springer: Dordrecht
5. Sarma KC, Adeli H (1997) Cost optimization of concrete structures. *J Struct Eng* 124:570-578
6. Lagaros ND (2014) A general purpose real-world structural design optimization computing platform. *Struct Multidiscip O* 49:1047-1066
7. Mergos PE (2018) Contribution to sustainable seismic design of reinforced concrete members through embodied CO<sub>2</sub> emissions optimization. *Struct Concrete* 19:454-462
8. Lagaros ND (2020) The environmental and economic impact of structural optimization. *Struct Multidiscip O* 49:1047-1066
9. Paya-Zaforteza I, Yepes V, Gonzalez-Vidoso F (2008) Hospitaler A. Multiobjective optimization of concrete frames by simulated annealing. *Comput-Aided Civ Inf* 23:596-610
10. Yeo D, Potra F (2015) Sustainable design of reinforced concrete structures through CO<sub>2</sub> emission optimization. *J Struct Eng* 141:B4014002
11. Martins A, Simões L, Negrão J, Lopes A (2020) Sensitivity analysis and optimum design of reinforced concrete frames according to Eurocode 2. *Eng Optimiz* 52:2011-2032
12. Mergos PE (2018) Seismic design of reinforced concrete frames for minimum embodied CO<sub>2</sub> emissions. *Energy Build* 162:177-186
13. Mergos PE (2021) Optimum design of 3D reinforced concrete building frames with the flower pollination algorithm. *J Build Eng* 44:102935
14. Mergos PE (2022) Surrogate-based optimum design of 3D reinforced concrete building frames to Eurocodes. *Developments in the Built Environment* 11:100079
15. Kaveh A, Ardebili SR (2023) Optimum design of 3D reinforced concrete frames using IPGO algorithm. *Structures* 48:1848-1855
16. Ganzerli S, Pantelides CP, Reaveley LD (2000) Performance-based design using structural optimization. *Earthq Eng Struct Dyn* 29: 1677-1690
17. Fragiadakis M, Papadrakakis M (2008) Performance-based optimum seismic design of reinforced concrete structures. *Earthq Eng Struct Dyn* 37: 825-844
18. Fragiadakis M, Lagaros ND (2011) An overview to structural seismic design optimization frameworks. *Comput Struct* 89:1155-1165
19. Mergos PE (2017) Optimum seismic design of reinforced concrete frames according to Eurocode 8 and fib Model Code 2010. *Earthq Eng Struct Dyn* 46:1181-1201
20. Mergos PE (2018c) Efficient optimum seismic design of reinforced concrete frames with nonlinear structural analysis procedures. *Struct Multidiscip O* 58:2565-2581
21. Mergos (2020) Minimum cost performance-based seismic design of reinforced concrete frames with pushover and nonlinear response history analysis. *Struct Concr* 21:599-609
22. Bruneau M, Chang SE, Eguchi RT, Lee GC, O'Rourke TD, Reinhorn AM, Shinozuka M, Tierney K, Wallace WA, Winterfeldt D (2003) A framework to quantitatively assess and enhance the seismic resilience of communities. *Earthq Spectra* 19: 733-752
23. Makris N (2019) Seismic isolation: Early history. *Earthq Eng Struct Dyn* 48:269-283
24. Li C, Chang K, Cao L, Huang Y (2021) A high performance hybrid passive base-isolated system. *Soil Dyn Earthq Eng* 143:106589
25. Cao L, Li C (2022) A high performance hybrid passive base-isolated system. *Struct Control Health Monit* 29:e2887
26. Naeim F, Kelly JM (1999) Design of seismic isolated structures: From theory to practice. Wiley

27. Clemente P, Marteli A (2019) Seismically isolated buildings in Italy: State of the art review and applications. *Soil Dyn Earthq Eng* 199: 471-487
28. Makris N (2014) A half-century of seismic isolation. *Earthq Struct* 7: 1187-1221
29. Housner GW (1963) The behaviour of the inverted pendulum structures during earthquakes. *Bull Seismol Soc Am* 5: 403-417
30. Psycharis IN, Jennings PC (1983) Rocking of slender rigid bodies allowed to uplift. *Earthq Eng Struct Dyn*: 11: 57-76
31. Dimitrakopoulos EG, DeJong MJ (2012) Revisiting the rocking block: closed-form solutions and similarity laws. *Proc R Soc A*: 468:2294-2318
32. Vassiliou MF, Mackie KR, Stojadinovic B (2014) Dynamic response analysis of solitary flexible rocking bodies: modeling and behaviour under pulse-like ground excitation. *Earthq Eng Struct Dyn*: 43: 1463-1481
33. Agalianos A, Psychari A, Vassiliou MF, Stojadinovic B, Anastasopoulos I (2017) Comparative assessment of two rocking isolation techniques for a motorway overpass bridges. *Front Built Environ* 3:47
34. Mander JB, Cheng CT (1997) Seismic resistance of bridge piers based on damage avoidance design. Technical Rep. NCEER, State Univ of New York at Buffalo
35. Marriott D, Pampanin S, Palermo A (2009) Quasi-static and pseudo-dynamic testing of unbonded post-tensioned rocking bridge piers with external replaceable dissipaters. *Earthq Eng Struct Dyn*: 38: 331-354
36. Giouvanidis AI, Dimitrakopoulos EG (2017) Seismic performance of rocking frames with flag-shaped hysteretic behaviour. *J Eng Mech* 143: 04017008
37. Kutter BL, Moore M, Hakhamaneshi M, Champion C (2016) Rationale for shallow foundation rocking provisions in ASCE 41-13. *Earthquake Spectra* 32:1097-1119
38. Antonellis G, Panagiotou M (2014) Seismic response of bridges with rocking foundations compared to fixed-base bridges at a near-fault site. *J Bridge Eng* 19:04014007-1
39. Mergos PE, Kawashima K (2005) Rocking isolation of a typical bridge pier on spread foundation. *J Earthq Eng* 9: Special Issue 2: 395-414
40. Anastasopoulos I, Gazetas G, Loli M, Apostolou M, Gerolymos N (2010) Soil failure can be used for seismic protection of structures. *Bull Earthq Eng* 8:309-326
41. Gelagoti F, Kourkoutis R, Anastasopoulos I, Gazetas G (2012) Rocking isolated frame structures: margins of safety against toppling collapse and simplified design approach. *Soil Dyn Earthq Eng* 32:87-102
42. Anastasopoulos I, Gelagoti F, Spyridaki A, Sideri J, Gazetas G (2014) Seismic rocking isolation of an asymmetric frame on spread footings. *J Geotech Geoenviron* 140:133-151
43. Hakhamaneshi M, Kutter BL, Andreas G, Gavras SM, Sivapalan G, Tsatsis A, Liu W, Sharma K, Pianese G, Kohno T, Deng L, Paolucci R, Anastasopoulos I, Gazetas G (2020) Database of rocking shallow foundation performance: Slow-cyclic and monotonic loading. *Earthq Spectra* 36:1585-1606
44. Deng L, Kutter BL, Kunath S (2014) Seismic design of rocking shallow foundations: Displacement-based methodology. *J Bridge Eng* 19:04014043
45. Millen M, Pampanin S, Cubrinovski M (2021) An integrated performance-based design framework for building-foundation systems. *Earthq Eng Struct Dyn* 50: 718-735
46. CEN (2004) Eurocode 8: Design of structures for earthquake resistance. Part 1: General rules, seismic actions and rules for buildings, Brussels: European Standard EN 1990-1
47. Kaethner SA, Burrige JA (2012) Embodied CO<sub>2</sub> of structural frames. *Structural Engineer* 90: 33-40.
48. Holland JH (1975) Adaptation in natural and artificial systems. An introductory analysis with application to biology, control and artificial intelligence. University of Michigan Press, Ann Arbor, MI
49. Deep K, Singh KP, Kansal ML, Mohan C (2009) A real coded genetic algorithm for solving integer and mixed integer optimization problems. *Appl Math Comput* 212:505-518
50. CEN (2000) Eurocode 2: Design of concrete structures. Part 1-1: General rules and rules for buildings, Brussels: European Standard EN 1992-1-1
51. CSI (2023) <https://www.csiamerica.com/products/etabs>
52. CSI (2023) <https://www.csiamerica.com/products/sap2000>
53. MathWorks (2022a) [https://uk.mathworks.com/products/matlab.html?s\\_tid=hp\\_products\\_matlab](https://uk.mathworks.com/products/matlab.html?s_tid=hp_products_matlab)